Published October 27, 2015

An Overview of CERES–Sorghum as Implemented in the Cropping System Model Version 4.5

J. W. White,* G. Alagarswamy, M. J. Ottman, C. H. Porter, U. Singh, and G. Hoogenboom

ABSTRACT

Sorghum [*Sorghum bicolor* (L.) Moench] is the fifth most important grain crop globally. It stands out for its diversity of plant types, end-uses, and roles in cropping systems. This diversity presents opportunities but also complicates evaluation of production options, especially under climate uncertainty. Ecophysiological models can dissect interacting effects of plant genotypes, crop management, and environment. We describe the sorghum module of the Cropping System Model (CSM) as implemented in the Decision Support System for Agrotechnology Transfer (DSSAT) to illustrate potential applications and suggest areas for model improvement. Crop growth is simulated based on radiation use efficiency. Development responds to temperature and photoperiod. Partitioning rules vary with growth stages, respecting mass balance and maintaining functional equilibrium between roots and shoots. Routines for climate, soil, crop management, and model controls are shared with other crops in CSM. Modeled responses for eight real-world and hypothetical cases are presented. These include growth under well-managed conditions, responses to row-spacing, population, sowing date, irrigation, defoliation, and increased atmospheric carbon dioxide concentration ($[CO_2]$), and a long-term sorghum and winter wheat (*Triticum aestivum* L.) rotation. Among traits and experiments considered, model accuracy was high for phenology ($r^2 = 0.96$, $P < 0.01$ for anthesis and $r^2 = 0.91$, $P < 0.01$ for maturity), moderate for grain yields (r^2 values from 0.30 to 0.52, $P < 0.01$), depending on the simulated experiments, and low for unit grain weight ($r^2 = 0.02$, not significant, NS) and leaf area index for forage sorghum ($r^2 = 0.18$, NS).

Published in Agron. J. 107:1987–2002 (2015)
doi:10.2134/agronj15.0102
Received 23 Feb. 2015
Accepted 31 May 2015
Supplemental material online

Valued for its heat and drought tolerance, sorghum is the fifth most important grain crop globally after wheat, rice (*Oryza sativa* L.), maize (*Zea mays* L.), and barley (*Hordeum vulgare* L.) (FAOSTAT, 2015). Among cereal crops, sorghum stands out for its diversity of plant types, cropping systems, growing environment, and end-uses (Dahlberg et al., 2011). Sorghum is variously grown to provide grain, forage, sugar, and bioenergy feedstocks, and crop architecture and other traits vary accordingly. While this diversity presents opportunities, it complicates attempts to assess potential impacts of innovations, especially as affected by climate uncertainty.

The CSM (Jones et al., 2003) as implemented in the DSSAT has submodels that allow simulation of more than 25 crop species, including sorghum (Hoogenboom et al., 2011). The sorghum submodule uses shared routines for model control (including input and output), soil physical and chemical processes, evapotranspiration, and all aspects of crop management including tillage, planting, fertilization, irrigation, mulching, and other practices. Eight subroutines describe sorghum-specific crop processes. The shared routines simplify model improvement and simulating cropping sequences and rotations with different crops and management practices. While based on the widely-used Crop Estimation through Resource and Environment Synthesis (CERES) approach for crop growth and development (Ritchie et al., 1998), the CSM sorghum source code has been extensively modified from prior versions (Alagarswamy et al., 1989; Ritchie and Alagarswamy, 1989a, 1989b). Recent modifications emphasized allowing more model parameters to be specified through the input files, which provide users greater control over phenology, partitioning, and environmental responses. Further modifications resolved issues related to modeling phenology and leaf number with emphasis on performance of photoperiod-sensitive germplasm. These changes were intended to improve the ability of the model to simulate forage and biomass germplasm and novel cropping practices.

J.W. White, USDA-ARS, USDA-ARS, Arid-Land, 21881 North Cardon Lane, Maricopa, AZ 85138; G. Alagarswamy, Center for Global Change and Earth Observations, 202 Manly Miles Building, 1405 S. Harrison Road, Michigan State Univ., East Lansing, MI 48824; M. J. Ottman, School of Plant Sciences, Univ. of Arizona, P.O. Box 210036, Tucson, AZ 85721; C.H. Porter, Dep. of Agricultural and Biological Engineering, Univ. of Florida, Gainesville, FL 32611; U. Singh, International Fertilizer Development Center, Complex F, Wilson Dam Highway, Muscle Shoals, AL 35661; G. Hoogenboom, AgWeatherNet Program, Washington State Univ., 24106 North Bunn Road, Prosser, WA 99350. *Corresponding author (Jeffrey.White@ars.usda.gov).

Abbreviations: CERES, Crop Estimation through Resource and Environment Synthesis; CSM, Cropping System Model; DSSAT, Decision Support System for Agrotechnology Transfer; RMSE, root mean squared error.

Using the earlier CERES–Sorghum model, Alagarswamy and Virmani (1996) analyzed risk associated with N applications for rainfed production at four locations in India and concluded that gross return was sensitive to rainfall reliability. Castrignanó et al. (1997) used lysimeter data to assess the performance of CERES–Sorghum in a dry, windy, and high radiation environment and noted problems with accurate estimation of soil evaporation. For dryland cropping in the Great Plains, Staggenborg and Vanderlip (2005) concluded that the CERES–Sorghum could provide agronomists with valuable insights regarding the feasibility of alterations in cropping systems before conducting field trials. CERES–Sorghum model was linked with a geographic information system (GIS) to assist with N fertilizer management in the Indian semiarid tropics (Singh et al., 1993).

More recent applications of versions of CSM–CERES–Sorghum range from guiding crop management to estimating potential impacts of climate change. Considering two soils representative of different farm types in Ghana, MacCarthy et al. (2010) simulated 15-yr series of sorghum crops and concluded that increased N fertilizer use would benefit crop water use efficiency as well as grain yield. In a study on effects of irrigation on sweet sorghum growth and ethanol yield, Miller and Ottman (2010) used CSM–CERES–Sorghum to estimate rooting depth for the irrigation scheduling. Under warming and increased atmospheric [CO_2], Grossi et al. (2013) concluded that the optimal sowing date for sorghum in Minas Gerais, Brazil, would become later mainly due to elevated [CO_2] improving crop response to water deficits. Testing the potential for adaptation through improved heat and drought tolerance in Mali, Singh et al. (2014) found that the relative benefits of heat and drought tolerance varied with the target location.

This paper describes CSM–CERES–Sorghum as implemented in DSSAT Version 4.5 with the objective of providing potential users an understanding of basic model assumptions and resulting modeled responses. Eight test cases illustrate the array of responses considered in the model. These include crop growth under near-potential productivity, cultivar response to planting date, crop response to irrigation regimes and to defoliation, crop and soil responses to tillage practices, and crop response to atmospheric [CO_2]. The examples were selected to suggest potential applications of the model, as well as to illustrate areas where improvements are needed. However, the examples do not include responses to temperature per se, N, excess moisture, and other factors that are considered in the model. White et al. (2005) reviewed the temperature responses of Version 4.0 of the CSM–CERES–Sorghum model.

MATERIALS AND METHODS

Model Description

Crop growth, including leaf area, is simulated using approaches first applied to wheat (and corn versions of CERES (Ritchie and Otter, 1985; Jones and Kiniry, 1986) and then adapted for sorghum and millet (Ritchie and Alagarswamy, 1989a, 1989b; Ritchie et al., 1998). The current version (Ver. 4.5.1.023) includes many features added through the general CSM framework (Jones et al., 2003) and specific improvements to the sorghum subroutines. The following sections describe basic features of the sorghum-specific subroutines. Table 1 lists the variables referenced along with definitions and units. Selected model equations are presented in Supplement A.

Crop Growth

Growth is simulated in the subroutine SG_GROSUB.FOR, which is called once a day from the main sorghum subroutine of CSM, SG_CERES.FOR. Daily net assimilation is estimated from the product of daily potential radiation use efficiency (RUE) and the photosynthetically active radiation (PAR) intercepted by the crop. Thus, the potential daily biomass production per plant, PCARB, is calculated as,

$$\text{PCARB} = \text{RUE} \times \text{PCO2} \times (\text{PAR}/\text{PLTPOP}) \times [1.0 - \text{EXP}(-\text{LIFAC} \times \text{LAI})]$$

where PCO2 is a factor to adjust RUE for atmospheric [CO_2], PLTPOP is plant population, which reduces the daily production to a per plant basis, and EXP(x) indicates exponentiation. The arguments of EXP(x) determine the fraction of PAR that is intercepted by the crop as a function of LIFAC, the light extinction coefficient, which is adjusted for effects of row spacing and population, and LAI, the leaf area index. LIFAC is assigned a larger value than would normally be used for the extinction coefficient because it includes interception by leaves and stems (Ritchie et al., 1998).

Various environmental stresses may reduce PCARB, giving the actual growth, CARBO, as

$$\text{CARBO} = \text{PCARB} \times \text{AMIN1}(\text{PRFT}, \text{SWFAC}, \text{NSTRES}) \times \text{SLPF}$$

where PRFT, SWFAC, NSTRES, and SLPF are factors scaled from 0 to 1 for temperature, plant available soil water, N deficit, and general soil fertility, respectively. AMIN1 is a function that returns the minimum value of its arguments. Thus, the effects of PRFT, SWFAC, and NSTRES depend on whichever factor is most limiting (Jones et al., 1986). PRFT is calculated using a weighted function of air temperature, TT,

$$\text{TT} = 0.25 \times \text{TMIN} + 0.75 \times \text{TMAX}$$

where TMIN and TMAX are the daily minimum and maximum air temperatures, respectively. A trapezoidal response is assumed with a base temperature (TBASE) of 8°C, a lower optimum (TOP1) of 20°C, an upper optimum (TOP2) of 40°C, and a maximum (TMAX in the context of cardinal temperatures) of 50°C.

Potential main stem leaf area (PLAN) is modeled on a per plant basis using the Gompertz function,

$$\text{PLAN} = \text{A} \times \text{EXP}[-10.34 \times \text{EXP}(-\text{PLAY} \times \text{CUMPH})]$$

where A is the maximum leaf area that a stem may attain (currently assumed to be invariant at 6000 cm^2 $plant^{-1}$), PLAY is a coefficient to indicate cultivar differences in leaf size. CUMPH is the cumulative leaf number (phyllochron), which is predicted from the daily thermal time increment (DTT) and the phyllochron interval (PHINT) as

Table 1. Variables referenced in describing basic processes used to simulate growth and development of sorghum in the CSM–CERES–Sorghum model.

Variable	Description	Units
A	Assumed maximum leaf area that a main stem may attain	cm^2 $plant^{-1}$
AGEFAC	Factor for N stress related to leaf ageing	(unitless)
CARBO	Assimilate available for plant growth (hence, plant growth rate)	g $plant^{-1}$
CUMP2	Total number of degree days since the end of juvenile phase	GDD†
CUMPH	Cumulated main stem (culm) leaf number (phyllochron)	leaves $plant^{-1}$
DLAYR(L)	Soil thickness in layer L	cm
DRGR	Root depth growth (extension) rate	cm soil depth GDD^{-1}
DTT	Daily thermal time increment	GDD
FSTR	Factor for cumulative nitrogen deficit ("fertility") during a given stage	(unitless)
G2	Scalar for partitioning of assimilates to the panicle	(unitless)
GDDE	Coleoptile extension rate	°Cday cm^{-1}
GPP	Grains per plant	number $plant^{-1}$
GRNWT	Grain weight per plant	g grain dry matter d^{-1}
GROLF	Leaf mass growth rate	g leaf dry matter $plant^{-1}$
GROPAN	Panicle mass growth rate	g panicle dry matter d^{-1}
GRORT	Root mass growth rate	g root dry matter $plant^{-1}$
GROSTM	Stem mass growth rate	g stem dry matter $plant^{-1}$
I	Hour of the day	h
L	Index for soil layers	(unitless)
LAI	Leaf area index.	(unitless)
LIFAC	Light interception factor for leaves and stems and which is adjusted for effects of row spacing and population	(unitless)
NSTRES	Factor describing effect of nitrogen deficit on photosynthesis	(unitless)
P1	Potential duration from emergence to end of juvenile phase	°C day
P2	Potential duration from end of juvenile phase to panicle initiation	°C day
P2O	Critical daylength above which development slows (short day response)	h
P2R	Photoperiod sensitivity as the extent to which development is delayed for each hour of photoperiod above P2O	°C day
P3	Duration from end of flag leaf expansion to anthesis	°C day
P4	Duration from anthesis to onset of grain filling	°C day
P5	Duration of grain-filling phase (onset of grain filling to physiological maturity)	°C day
P9	Net duration from sowing to emergence	°C day
PAF	Factor to slow grain filling as the crop approaches maturity	(unitless)
PANTH	Duration from panicle initiation to anthesis	°C day
PANWT	Panicle mass	g panicle dry matter $plant^{-1}$
PAR	Photosynthetically active radiation	MJ m^{-2} d^{-1}
PC	Factor that increases effect of PHINT linearly with CUMPH	(unitless)
PCARB	Potential daily biomass production per plant	g $plant^{-1}$ d^{-1}
PCO2	Factor to adjust RUE for atmospheric CO2 concentration	(unitless)
PGC	Cultivar-specific factor PGC for partitioning of assimilate to grain, derived from G2	(unitless)
PHINT	Phyllochron interval	°C day $leaf^{-1}$
PLAG	Growth in leaf area per plant for 1 d	cm^2 $plant^{-1}$ d^{-1}
PLAN	Potential main stem leaf area per plant basis	cm^2 $plant^{-1}$
PLAO	Leaf area from the previous day	cm^2 $plant^{-1}$
PLAY	Factor to indicate cultivar differences in leaf size	(unitless)
PLTPOP	Plant population	plants m^{-2}
PRFT	Factor describing effect of temperature on photosynthesis	(unitless)
RATEIN	Rate of floral induction	°C day
RGFILL	Rate of grain filling	mg d^{-1}
RLDF(L)	Factor to determine relative root distribution over soil layers	(unitless)
RLNEW	Length of newly-formed roots	cm
RLWR	Root length to weight ratio as specified as a species-level parameter.	cm g^{-1}
RNFAC	Effect of soil mineral nitrogen availability on root growth	(unitless)

(continued)

Table 1 (continued).

Variable	Description	Units
RTDEP	Rooting depth (RTDEP)	cm
RTPC	Root growth partitioning coefficient	(unitless)
RUE	Radiation use efficiency based on PAR	g plant dry matter MJ^{-1}
SDEPTH	Depth of sowing	cm
SHF(L)	Root distribution factor that is input from the soil profile description	(unitless)
SLPF	Factor describing effect of general soil fertility on photosynthesis	(unitless)
STMWT	Stem mass	g stem dry matter $plant^{-1}$
STPC	Stem growth partitioning coefficient	(unitless)
SUMDTT	Summation of daily thermal time (DTT)	°C day
SWDF	Soil water deficit	(unitless)
SWFAC	Factor describing effect of plant available soil water on photosynthesis	(unitless)
TBASE	Base temperature (TBASE) for development, assuming a segmented linear response	°C
TC1	Factor to adjust tiller-borne leaves as affected by solar radiation and temperature	(unitless)
TC2	Factor to adjust tiller-borne leaves as affected by plant population	(unitless)
TEMF	Represents temperature effect on leaf expansion	(unitless)
TH	Air temperature at hour I	°C
TI	Potential number of tiller-borne leaves formed per day	number d^{-1}
TILN	Tiller number (counting main stem as one tiller)	number $plant^{-1}$
TMAX	Maximum value of daily air temperature. Also, cardinal temperature above which no growth or development occurs.	°C
TMIN	Minimum value of daily air temperature	°C
TOPT	Optimal temperature for development, assuming a segmented linear response	°C
TOP1	Lower optimum for development, assuming a trapezoidal response	°C
TOP2	Upper optimum for development, assuming a trapezoidal response	°C
TSIZE	Relative size of tillers as compared to main culm	(unitless)
TURFAC	Factor for water stress due to insufficient uptake under soil moisture deficits or to excess soil moisture	(unitless)
TWILEN	Daylength estimated based on civil twilight (center of the sun is 6° below the horizon)	H
WSTR	Factor for cumulative water deficit ("fertility") during a given stage	(unitless)

† GDD indicates units for growing degree days.

$$CUMPH = CUMPH + DTT/PHINT$$

Adverse environmental conditions can reduce potential daily leaf expansion, PLAN-PLAO, where PLAO is the leaf area from the previous day. Thus, the actual daily leaf area increment, PLAG, is calculated as

$$PLAG = (PLAN - PLAO) \times AMIN1(TURFAC, TEMF, AGEFAC)$$

where TURFAC is a factor for water deficits, TEMF represents temperature effects, and AGEFAC accounts for leaf ageing related to N stress. If tillers are present, PLAG is further adjusted for tiller-borne leaf area (explained under Tillering).

Leaf area may decrease due to senescence or pest damage. Senescence is driven by the most limiting of factors for effects of water deficit, N deficit, light competition, and temperature in a manner similar to that described for CERES–Maize (Jones et al., 1986).

Phenology

Sorghum phenology is modeled by recognizing a series of phases delimited by stages that include seedling emergence, end of juvenile phase (phase when plants are insensitive to photoperiod; Alagarswamy et al., 1998), panicle initiation, end of leaf expansion, anthesis, and physiological maturity (Table 2). Phenology is simulated in the routine SG_PHENOL.FOR. Mathematically, the duration of a given phase is estimated by integrating a phase-specific potential rate over calendar time. The integrations for the various stages are coded as summations of daily thermal time, DTT (equivalent to heat units or growing degree days), giving SUMDTT. A phase is completed when the integral over the phase reaches a target value, specified by cultivar-specific parameters (e.g., P1, P3, and PANTH in Table 3). Cardinal temperatures for estimating DTT are specified in a file of parameters that are defined at the level of crop ecotypes (Table 3). Currently, a segmented linear model is used for all ecotypes, assuming a TBASE of 8°C and TOPT of 34°C for vegetative and reproductive phases (Ritchie and Alagarswamy, 1989a).

The actual calculation of DTT considers whether air temperature was less than TBASE or exceeded TOPT, by reconstructing a diurnal temperature regime from TMIN and TMAX. For TMIN > TBASE and TMAX < TOPT, the daily mean temperature is used and is estimated as the average of TMIN and TMAX,

$$DTT = [(TMAX + TMIN)/2.0] - TBASE$$

If TMIN < TBASE or TMAX > TOPT, hourly temperatures (TH) are estimated using a sine curve to interpolate between the extremes,

Table 2. Developmental stages recognized in CSM–CERES–Sorghum model code. The growth stages are as specified by Vanderlip (1993).

Name	Primarily affected by	Growth stage	Stage in model code
Sowing date			7
Germination	Soil moisture		8
Emergence	Temperature	0	9
End of juvenile phase	Temperature		1
Panicle initiation	Temperature, photoperiod		2
End of flag leaf expansion	Temperature		3
Anthesis	Temperature	6	
Beginning grain fill	Temperature		4
Physiological maturity	Temperature	9	5
Harvest			6

Table 3. Model parameters used to represent differences among cultivars and ecotypes in CSM–CERES–Sorghum.

Parameter	Description	Units	Default value
Cultivar			
P1	Thermal time from seedling emergence to the end of the juvenile phase during which the plant is not responsive to changes in photoperiod	°C day	180
P2	Thermal time from the end of the juvenile stage to tassel initiation under short days	°C day	400
P2O	Critical photoperiod or the longest day length at which development occurs at a maximum rate. At values higher than P2O, the rate of development is reduced	hours	12.74
P2R	Extent to which phasic development leading to panicle initiation is delayed for each hour increase in photoperiod above P2O	°C day h^{-1}	40
PANTH	Thermal time from the end of tassel initiation to anthesis	°C day	300
P3	Thermal time from to end of flag leaf expansion to anthesis	°C day	50
P4	Thermal time from anthesis to beginning grain filling	°C day	70
P5	Thermal time from beginning of grain filling to physiological maturity	°C day	600
PHINT	Phyllochron interval (inverse of leaf appearance rate)	°C day	49
G1	Scalar for relative leaf size		5
G2	Scalar for partitioning of assimilates to the panicle (head).		6
PSAT†	Critical photoperiod below which development is not delayed (optional)	hours	13.75
PBASE†	Ceiling photoperiod above which development is delayed indefinitely (optional)	hours	12.85
Ecotype			
ECO#	Code linking an ecotype to a cultivar (links to cultivar file)		(none)
TBASE	Base temperature below which no development occurs	°C	8
TOPT	Temperature at which maximum development occurs for vegetative stages	°C	34
ROPT	Temperature at which maximum development occurs for reproductive stages	°C	34
GDDE	"Growing degree days" (thermal time) per cm seed depth required for emergence	°C day cm^{-1}	6
RUE	Radiation use efficiency based on total plant (shoot and root) and photosynthetically active radiation (PAR)	g plant dry matter MJ^{-1}	3.2
KCAN	Canopy light extinction coefficient for daily PAR		0.85
STPC	Partitioning to stem growth as a fraction of potential leaf growth		0.6
RTPC	Partitioning to root growth as a fraction of available carbohydrates		0.25
TILFC	Tillering factor (0.0 indicates no tillering and 1.0 is full tillering)		0.00

† Coefficients included to allow use of an alternate model for effects of photoperiod.

$$TH = [(TMAX + TMIN)/2.0] + [(TMAX - TMIN)/2.0] \times SIN(I \times 3.14/12.0)$$

where I represents the hour of the day. The hourly increments of thermal time are estimated using TBASE and TMAX and summed to give DTT.

The actual temperatures used to calculate DTT are adjusted from the air temperature to better represent growing point (crown) temperature, which is assumed closer to soil temperature during early development (when the leaf tip number is less than or equal to 10 or the panicle has not yet been initiated).

Upon planting, 50 units of thermal time (°C-day, formerly termed "growing degree days" or "GDD") are required for germination. Time from germination to emergence is calculated from a coleoptile extension rate (GDDE) and the sowing depth (SDEPTH). Thus, the net duration from sowing to emergence, P9, is

$$P9 = 50.0 + GDDE \times SDEPTH$$

The end of the juvenile phase is reached when SUMDTT is equal to or greater than the corresponding phase duration, P1.

The duration from end of juvenile phase to panicle initiation is a function of temperature and daylength, with the potential duration specified by the cultivar coefficient P2. The effect of daylength is calculated as the delay due to the number of hours above the critical daylength, P2O, which is also cultivar specific. The delay is proportional to the cultivar specific photoperiod sensitivity, P2R. Because photoperiod responses are sensitive to low light intensities, daylength is estimated based on civil twilight (center of the sun is 6° below the horizon), represented as TWILEN (Francis, 1970). The rate of floral induction (RATEIN) is evaluated daily as

$$RATEIN = P2 + [P2R \times (TWILEN - P2O)]$$

Panicle initiation occurs when the total number of degree days since the end of juvenile phase (CUMP2) is greater than or equal to RATEIN.

The duration from panicle initiation to the end of flag leaf expansion is calculated as the difference between the duration from panicle initiation to anthesis (PANTH) and the duration from end of flag leaf expansion to anthesis (P3). Anthesis date thus is determined by PANTH. Onset of grain filling is referenced from the anthesis date and occurs when SUMDTT reaches P4. The final phase is the grain-filling period, which ends when SUMDTT attains P5. Physiological maturity is assumed to occur the next day if DTT or SUMDTT is greater than 2°C day. At maturity, the crop simulation ends. P2, P2R, P2O, PANTH, P3, P4, and P5 are cultivar-specific inputs (Table 3).

Partitioning

Partitioning of assimilate into different organs is governed by stage-specific rules that are similar to those defined for CERES–Maize (Jones et al., 1986). Two fundamental principles are to maintain the daily assimilate balance (i.e., that daily growth or senescence of all organs sums to CARBO) and to maintain the functional equilibrium between root–shoot partitioning (Brouwer, 1983).

In stage 1 (juvenile phase), only leaves and roots grow. The leaf area growth rate (PLAG) is converted to a mass growth rate (GROLF) via the specific leaf weight. Any remaining assimilate, CARBO, is allocated to roots with a constraint that if GRORT is less than RTPC × CARBO, where RTPC is a root partitioning coefficient defined for crop ecotypes, then GRORT is set equal to RTPC × CARBO, and GROLF and PLAG are reduced proportionally to maintain assimilate balance. The default value of RTPC is 0.25, which is consistent with estimates reviewed by Lambers (1987) for multiple species based on evidence from $^{14}CO_2$ studies.

In stage 2 (photoperiod sensitive phase up to panicle initiation), leaf area per plant is again used to estimate potential leaf growth. In this phase, tiller leaf area is considered. Stem growth (GROSTM) is allowed as

$$GROSTM = GROLF \times STPC$$

where STPC is a stem partitioning coefficient defined as an ecotype coefficient. An initial estimate of root growth is given as

$$GRORT = (CARBO - GROLF) - GROSTM$$

If GROLF plus GROSTM is >1.0 – GRORT, then GROLF and GROSTM are reduced proportionately to ensure assimilate balance.

Stage 3 lasts from panicle initiation to the end of flag leaf expansion, which is measured in thermal time as the difference PANTH– P3, where PANTH is the thermal time from end of tassel initiation to anthesis, and P3 is the thermal time from end of flag leaf expansion to anthesis. Both P3 and PANTH are cultivar-specific (Table 3). An initial value of GROLF is again estimated from PLAG (including tiller-borne leaves). It is then used to estimate stem partitioning as

$$GROSTM = GROLF \times \{STPC + 0.8 \times [SUMDTT/(PANTH - P3)]^{**}2\}$$

The term summed with STPC increases partitioning to stem mass as the crop approaches the end of leaf growth. GRORT is calculated similarly to the previous phases, and if needed, GRORT, GROSTM, and GROLF are reduced proportionately to ensure assimilate balance.

Stage 4, the end of leaf expansion to onset of grain filling, starts when leaf growth ceases. During this phase, CARBO is allocated only to stems and roots. Potential stem growth increases linearly with DTT, with adjustments for tiller number and size and for water deficit and temperature effects. However, a minimum of 0.08 × CARBO must go to roots. The reduction in partitioning to roots reflects the decrease in root growth before panicle emergence as described by Blum and Arkin (1984).

With the onset of the grain-filling period (stage 5), an initial panicle mass (PANWT) is established as

$$PANWT = STMWT \times G2 \times 0.05$$

where STMWT is the stem mass, and G2 is a cultivar-specific scalar for partitioning of assimilate to the panicle (Table 3), which is required to accommodate the large variation in panicle size in sorghum germplasm (e.g., Rami et al., 1998). Panicle growth and grain formation are described subsequently.

Tillering

Tiller formation has a large impact on growth and yield in sorghum (Kim et al., 2010). The model simulates tiller appearance and growth following the approach used for CERES–Wheat (Ritchie and Godwin, 2000) but with modifications specific to sorghum. The number of tillers and balance between tiller and main culm growth vary with developmental stage, water stress, plant population, and other factors.

Tillers can form up to time of panicle initiation. The smaller of the two factors for tiller formation, TC1 and TC2, are used to calculate TILN, the number of tillers per plant,

$$TILN = TILN + (TI \times AMIN1(TC1, TC2) \times TURFAC)$$

TI is the potential number of tiller-borne leaves formed per day,

$$TI = DTT/(PHINT \times PC)$$

where PC is a factor that increases effect of PHINT linearly with CUMPH, for CUMPH < 5. TC1 varies with the quotient of daily solar radiation and temperature, which is used to represent the balance between potential crop growth and development (Nix, 1976). TC2 accounts for effects of competition,

$$TC2 = 6.25E\text{-}5 \times (40.0 - PLTPOP \times TILN)^{**}3$$

with an assumed maximum of 40 culms m^{-2}.

To obtain the daily growth in tiller leaf area (PLAGT), the potential leaf area of tillers (PLATN) is first estimated as a function of TLIN and CUMPH growth. Subtracting the previous day's potential tiller leaf area, the growth is

$$PLAGT = (PLATN - PLATO) \times AMIN1(TURFAC, TEMF, AGEFAC)$$

again with a potential effect of stress factors on growth. The value of PLAGT is summed with the estimate of main stem leaf area growth, PLAG, to give the current day's net leaf growth.

During stages 4 and 5, the size of tillers, TSIZE, is used to scale initial partitioning to stems and panicles. TSIZE is reduced with plant population,

$$TSIZE = EXP[-0.15 \times (PLTPOP - 2.0)]$$

Panicle Growth and Grain Formation

Reproductive growth is simulated during stage 5. A single-grain growth rate is first calculated, thus assuming that all grains grow at the same rate. First a relative grain-filling rate, RGFILL, scaled from 0 to 1, is calculated as a function of mean air temperature, assuming a trapezoidal response with a TBASE of 7°C, end-points of the optimal range of 22 and 48°C, and zero growth at 50°C.

Panicle growth rate, GROPAN, is then estimated as the product of RGFILL, the cultivar-specific factor PGC for partitioning of assimilate to grain (derived from G2 in Table 3), a factor that slows grain filling as the crop approaches maturity (PAF), the relative size of all culms including tillers, and N and water stress factors,

$$GROPAN = RGFILL \times PGC \times PAF \times (1.0 + (TILN - 1.) \times TSIZE) \times AMIN1(FSTR,WSTR)$$

where FSTR and WSTR, respectively, are the cumulative N and water stress factors for the current developmental phase. Stem growth is then defined as

$$GROSTM = CARBO - GROPAN$$

and root growth is set to 0.

The number of grains per plant (GPP) is calculated at the onset of grain filling (stage 5) as a linear function of crop growth rate from panicle initiation to anthesis based on concepts of Edmeades and Daynard (1979) that were developed for maize. Grain weight per plant (GRNWT) is assumed to be 0.8 of PANWT. Unit grain weight is obtained by dividing GRNWT by GPP.

Root Length Growth

A vertical profile of root length density through the soil is needed to calculate root water uptake. To model the distribution of roots in the soil, newly created root mass is converted to root length and distributed to different depths in the subroutine SG_ROOTGR, following approaches used in CERES–Maize (Jones et al., 1986) and similar to the approach of Robertson et al. (1993). To account for biomass losses due to root exudates and senescence (Lambers, 1987), it is assumed that only 60% of the biomass partitioned to the roots becomes root mass. Furthermore, 0.5% of the root mass is assumed to be lost daily through respiration. The conversion of new root mass, GRORT, to new length, RLNEW, is calculated as

$$RLNEW = GRORT \times RLWR \times PLTPOP$$

where RLWR is the root length to weight ratio specified as a species-level parameter.

Because the model assumes a one-dimensional soil profile, the roots are equally distributed throughout the soil for a given layer. Rooting depth (RTDEP) increases proportionally with daily thermal time (DTT) and a downward growth rate, DRGR,

$$RTDEP = RTDEP + DTT \times DRGR \times SQRT[SHF(L) \times AMIN1(SWFAC \times 2.0,SWDF)]$$

where the factor SHF(L) is a root distribution factor for input from the soil profile description, and SWFAC and SWDF represent plant and soil water deficit effects, respectively. If CUMDTT < 275, DRGR is 0.1 cm °C d^{-1}; otherwise, DRGR is 0.2 cm °C d^{-1}.

The vertical distribution of the roots up to the current RTDEP is evaluated by calculating a relative root length density factor [RLDF(L)] at each soil depth increment [DLAYR(L)],

$$RLDF(L) = AMIN1(SWDF, RNFAC) \times SHF(L) \times DLAYR(L)$$

where RNFAC is a factor that represents the effect of available soil mineral N on root growth and SHF(L) is a soil "hospitality" factor for each layer (L) that varies from 0 to 1.

Water, Nutrient, and Organic Carbon Dynamics

Soil water, N, and organic C dynamics and their interactions with crop management including tillage (White et al., 2010) and pest damage (Boote et al., 1983) are determined in subroutines that are shared among all crops represented in CSM. Detailed descriptions of the soil water, N, and C balance dynamics are found in Ritchie (1998) and Godwin and Singh (1998).

Simulations

All simulations were conducted using version 4.5.1.023 of CSM as provided in DSSAT4.5 (Hoogenboom et al., 2011). In accordance with normal use of CSM, cultivar and ecotype coefficients were adjusted as needed to represent performance of specific cultivars or hybrids (Boote, 1999). This primarily involved iterative changes to cultivar or ecotype coefficients for phase durations and photoperiod sensitivity (Table 3) to match measured and simulated crop phenology. Species-level coefficients were not modified except as noted to demonstrate the model response to [CO_2].

Data Sources

Model input files describing crop management, soil profile descriptions, and weather data were mainly prepared using tools in DSSAT 4.5. Experiment details are summarized in Supplement B, and soil profiles used are given in DSSAT format in Supplement C. All datasets used are available on request to the corresponding author.

Growth and Partitioning

Data for sorghum growth and development under favorable moisture and N availability were obtained from Pachta (2007). The hybrid Pioneer 87G57[1] was planted on 5 June 2006 at Manhattan, KS, (39.22°N, 96.58°W; 299 m above sea level) in a soil classified as a Smolan series (fine, smectitic, mesic Typic Argiudoll). The row spacing was 0.76 m, with a population of 13.9 plants m^{-2}. Although 440 mm of rainfall fell between planting and harvest, and the actual experiment received 112 kg N ha^{-1} as urea and ammonium nitrate, the experiment was simulated assuming no water or N deficits due to lack of data on initial soil water and N status.

Row Spacing and Plant Population

To examine responses to row-spacing and plant population, a series of three rainfed trials at the USDA Conservation and Production Research Lab in Bushland, TX, (35.19° N, 102.08° W; elev. 1170 m) were simulated (Jones and Johnson, 1991). The soil was a slowly permeable Pullman clay loam (fine, mixed, thermic Torrertic Paleustoll). The hybrid DeKalb-46 was planted on 26 June 1986, 11 June 1987, and 7 June 1988. Row spacings and densities were 0.76 m by 8 or 16 plants m^{-2} and 1.52 m by 4 or 8 plants m^{-2}. Actual densities used in the simulations corresponded to population counts at 10 to 14 d after emergence. No fertilizer was applied. Variables reported in Jones and Johnson (1991) included maximum LAI, aboveground DM at harvest, grain yield, and effective tiller number.

Planting Date

Ottman et al. (1998) described a planting date study at Maricopa, AZ, (33.07° N; 111.97° W; 361 m above sea level) where 17 commercial hybrids were sown at seven dates ranging from 19 Mar. to 30 July 1997. The soil was a Pima clay loam (fine-loamy, mixed, hyperthermic Typic Natriargid). The crop was irrigated and fertilized to avoid stress. Days to anthesis and to maturity were evaluated visually. Duration of grain filling was calculated as the time from anthesis to maturity. We simulated the response of five Cargill hybrids that represent a range of maturities (Car-577, Car-727, Car-737, Car-837, and Car-877).

Irrigation

Erie et al. (1959) described results from an irrigation management study where two grain sorghum cultivars (Double Dwarf-38 and the hybrid RS-610) were tested under eight irrigation regimes and three levels of added N, 0, 112, and 224 kg ha^{-1}. The experiment was sown on 26 June 1958 at Mesa, AZ, (33.42° N; 111.82° W; 376 m above sea level) in a soil of the Laveen series and classified as a coarse-loamy, mixed, thermic Typic Calciorthid. The design was a split-split plot with six replications. Irrigation was the main plot, cultivar was the subplot, and N was the sub-subplot. The eight irrigation regimes involved flooding diked plots ("borders") and emphasized timing of two to six irrigations following a pre-plant irrigation on 17 June. Lesser corn borer (*Elasmopalpus lignosellus*) reduced yields in three treatments where a post-emergence irrigation was not provided. These treatments were simulated but analyzed separately from the other five treatments.

Data for sorghum forage growth and development were obtained from a 2-yr irrigation management study at Maricopa, AZ, (Ottman, 2010 and unpublished data, 2010) on a Casa Grande sandy loam soil (fine-loamy, mixed, hyperthermic Typic Natrargid). The hybrid Richardson Seeds Silo 700D was planted on 7 July 2009 and 9 July 2010 in 1 m-wide rows with a population of 23.7 plants m^{-2}. Nitrogen was provided as urea, with 112 kg ha^{-1} at planting and 112 kg ha^{-1} 30 d after planting. The crop was irrigated at planting and at nine additional times to provide 100, 70, 50, or 25% of estimated potential evapotranspiration. Anthesis date, forage yield, final stem number, leaf number, and LAI were measured.

Artificial Defoliation

Models are often used to assess potential losses due to defoliation related to insect pests, diseases, or hail damage, so modeled crop response to defoliation was assessed using four experiments conducted at Manhattan, KS, in 1958 and 1959 that were described by Stickler and Pauli (1961). The crops were sown in 1 m-wide rows with a population of 6.4 plants m^{-2}. Sorghum cultivar Midland was subjected to seven levels of defoliation at late boot stage. The treatments were a control, removal of alternate leaves, complete leaf removal, and leaving only leaf 1, 2, 5, 7, or 9. The cultivar Plainsman was subjected to five levels of defoliation either at boot stage or anthesis. Treatments involved removal of alternate leaves, the upper or lower half of all leaves, or all leaves. No dates for sowing were reported, so 10 June was assumed for both years. Similarly, dates of defoliation were given as growth stages, so dates of referenced stages were estimated assuming that booting occurred 10 d before anthesis. Experiments were assumed to be rainfed and to receive 110 kg ha^{-1} of N at sowing.

The cultivar coefficients for Midland and Plainsman were estimated from independent experiments, and soil conditions were assumed similar to those used in the growth study (Pachta, 2007). Defoliation treatments were imposed using the pest management routines of CSM whereby the model

[1]Mention of trade names or commercial products in this publication is solely for the purpose of providing specific information and does not imply recommendation or endorsement by the U.S. Department of Agriculture.

converts levels of leaf area reduction to equivalent losses of leaf mass and N (Boote et al., 1983; Teng et al., 1998).

Tillage and Soil Organic Carbon

To illustrate modeling of crop response to tillage, a hypothetical sorghum–winter wheat (rotation was simulated at Bushland, TX, from 1958 to 1999. This rotation involved two fallow periods, one following each crop, and thus took 3 yr per cycle. The 42-yr sequence was initiated twice, once starting with sorghum and once with wheat. Initial soil conditions and crop management for sorghum were simulated as for the row-spacing and population experiment except that a constant planting date of 10 June was used, the hybrid was assumed to be Cargill-727, which had a slightly longer growth cycle than DeKalb-46. The population was specified as 16 plants m^{-2} with a 76 cm row spacing. Wheat cultivar Newton was sown on 6 July at a population of 150 plants m^{-2} with a 15 cm row spacing. Based on Unger (1994), no fertilizer was provided for either crop. Soil organic C dynamics were simulated using the CENTURY model as adapted to CSM (Gijsman et al., 2002; Porter et al., 2010). Pools were initialized by assuming that the field had been under cultivation for 20 yr.

Response to Atmospheric Carbon Dioxide

The sensitivities of crop growth and water use to [CO_2] were illustrated by simulating a rainfed crop at Manhattan, KS, assuming the same conditions and management as the 2006 single-treatment experiment used to characterize basic growth responses. However, in this case water and N dynamics were simulated. The primary effect of [CO_2] is through the factor PCO2, which modifies RUE. PCO2 increases from a value of 0.95 at 330 μL L^{-1} [CO_2], 1.00 at 440 μL L^{-1}, 1.04 at 660 μL L^{-1} and 1.07 at 990 μL L^{-1}, following the assumption that sorghum has a response similar to that described for maize (Curry et al., 1990) and accounting for responses reviewed by Hatfield et al. (2008). To assess the impact of PCO2, three alternative response functions were tested. For these, the effect of [CO_2] on RUE was increased by proportional factors resulting in no response to 330 μL L^{-1} of [CO_2] to 1.05, 1.1 or 1.2 times, respectively, the default response at 990 μL L^{-1} [CO_2].

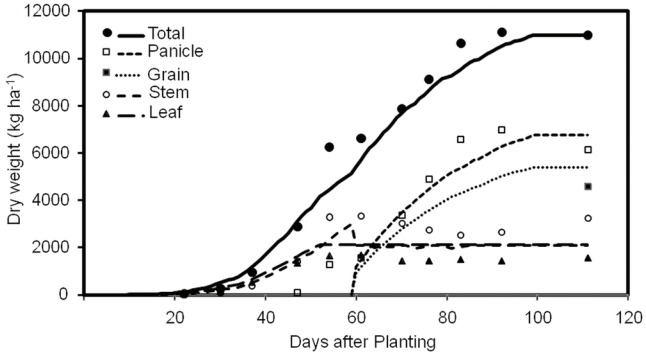

Fig. 1. Comparison of simulated (lines) vs. measured (points) total, panicle, grain, stem, and leaf dry weights over time for a rainfed sorghum crop grown in 2006 at Manhattan, KS.

Table 4. Summary of evaluations of simulation accuracy for datasets that included measured values.

Dataset	Variable	Units	N	r^2	RMSE†	Relative RMSE	Mean difference	Slope
Growth and partitioning	Leaf weight	kg ha^{-1}	11	0.98**	482	0.41	421	1.34 (0.07)‡
(Manhattan, KS, Fig. 1)	Stem weight	kg ha^{-1}	11	0.96**	739	0.35	–539	0.63 (0.05)
	Grain yield	kg ha^{-1}	1	na§	789	0.17	789	na
	Total aboveground weight	kg ha^{-1}	11	0.98**	761	0.12	–416	0.92 (0.04)
	Panicle weight	kg ha^{-1}	6	0.94**	728	0.19	–409	0.89 (0.14)
Row spacing and plant population	Maximum leaf area index		12	0.86**	0.49	0.22	–0.38	0.79 (0.10)
(Bushland, TX, Fig. 2)	Grain yield	kg ha^{-1}	12	0.51**	730	0.19	–2	0.50 (0.16)
	Total aboveground weight	kg ha^{-1}	12	0.40**	2290	0.25	–1480	0.56 (0.22)
	Tiller number	m^{-2}	12	0.45**	2.8	0.38	–0.20	0.46 (0.16)
Planting date	Days to anthesis	d	34	0.96**	3.9	0.06	0.1	1.08 (0.04)
(Maricopa, AZ, Fig. 3)	Days to maturity	d	34	0.91**	6.6	0.08	0.0	1.20 (0.07)
	Duration of grain filling	d	34	0.34**	5.0	0.25	–0.1	0.74 (0.18)
Irrigation at Mesa, AZ	Grain yield, normal plots	kg ha^{-1}	30	0.30**	270	0.07	30	0.59 (0.17)
(Fig. 4)	Grain yield, corn borer damage	kg ha^{-1}	18	0.52**	1390	0.38	1120	1.26 (0.31)
Irrigation at Maricopa, AZ	Forage yield	kg ha^{-1}	8	0.76**	2100	0.17	–20	1.52 (0.35)
(Fig. 5)	Leaf area index at harvest		8	0.18	1.45	0.33	0.8	0.67 (0.59)
Defoliation	Grain yield	kg ha^{-1}	40	0.35**	2320	1.28	480	0.39 (0.09)
(Manhattan, KS, Fig. 6)	Unit grain weight	mg $seed^{-1}$	40	0.02	22.1	1.64	8.3	–0.14 (0.15)

** Significant at the $P < 0.01$ level.

† RMSE, root mean squared error.

‡ Number in parentheses is the standard error of the estimate of the slope.

§ na, not applicable.

Statistical Analyses

Processing of model outputs, including calculation of means, estimations of linear regressions, and preparation of graphs, was conducted using the SAS version 9.2 software (SAS Institute Inc., Cary, NC). Simulation accuracy was evaluated mainly based on r^2 values, root mean squared error (RMSE), relative RMSE (with mean of measured values as the denominator), mean difference (as mean of simulated less mean of measured values), and the slope of the regression of measured vs. simulated values.

RESULTS

Growth and Partitioning

The ability of the model to reproduce overall patterns of growth is indicated for a rainfed crop at Manhattan, KS, where dry matter is given as stem, leaf, grain, and total weights (Fig. 1). The abrupt drop in stem weight at approximately 55 d corresponded to the allocation of stem weight to panicle weight. Leaf weight was overestimated, but stem was underestimated by a similar amount (mean deviation of 420 kg ha^{-1} for leaf and −540 kg ha^{-1} for stem; Table 4). Grain, panicle, and total weights showed acceptable agreement as judged by relative RMSE (Table 4).

Row Spacing and Plant Population

In the row spacing by population study at Bushland, TX, the trends for simulated and observed data (Fig. 2 and Table 4) showed good agreement for maximum LAI ($r^2 = 0.86$, $P < 0.001$) and moderate agreement for total aboveground dry weight ($r^2 = 0.40$, $P < 0.05$), grain yield ($r^2 = 0.51$, $P < 0.01$), and number of grain-bearing tillers ($r^2 = 0.45$, $P < 0.05$). For all four variables, the model appeared to underestimate values at the 1.52 m row spacing. Low values of regression slopes (Table 4) further suggest that the model is not sensitive enough to row spacing or populations.

Planting Date

The ability of the model to simulate crop phenology is indicated by a comparison of five hybrids planted at Maricopa, AZ, over seven dates from 19 Mar. to 30 July 1997 (Fig. 3 and Table 4). The wide range of planting dates exposed crops to daily mean temperatures from 10 to 34°C. Agreement between measured and simulated days to anthesis and to maturity was good ($r^2 = 0.96$, $P < 0.001$ and $r^2 = 0.91$, $P < 0.001$, respectively), but duration of grain filling showed discrepancies as large as 6 d ($r^2 = 0.34$, $P < 0.001$), which seems large relative to the measured mean duration of 20 d (Fig. 3C).

Irrigation

For the irrigation study at Mesa, AZ, agreement between measured and simulated grain yield was generally good for the five treatments that Erie et al. (1959) reported as being unaffected by corn borer ($r^2 = 0.30$, $P < 0.01$ and RMSE = 160 kg ha^{-1}; Fig. 4 and Table 4). The three irrigation treatments with corn borer damage had low measured yields but still showed a positive trend with simulated yield, apparently related to cultivar Double

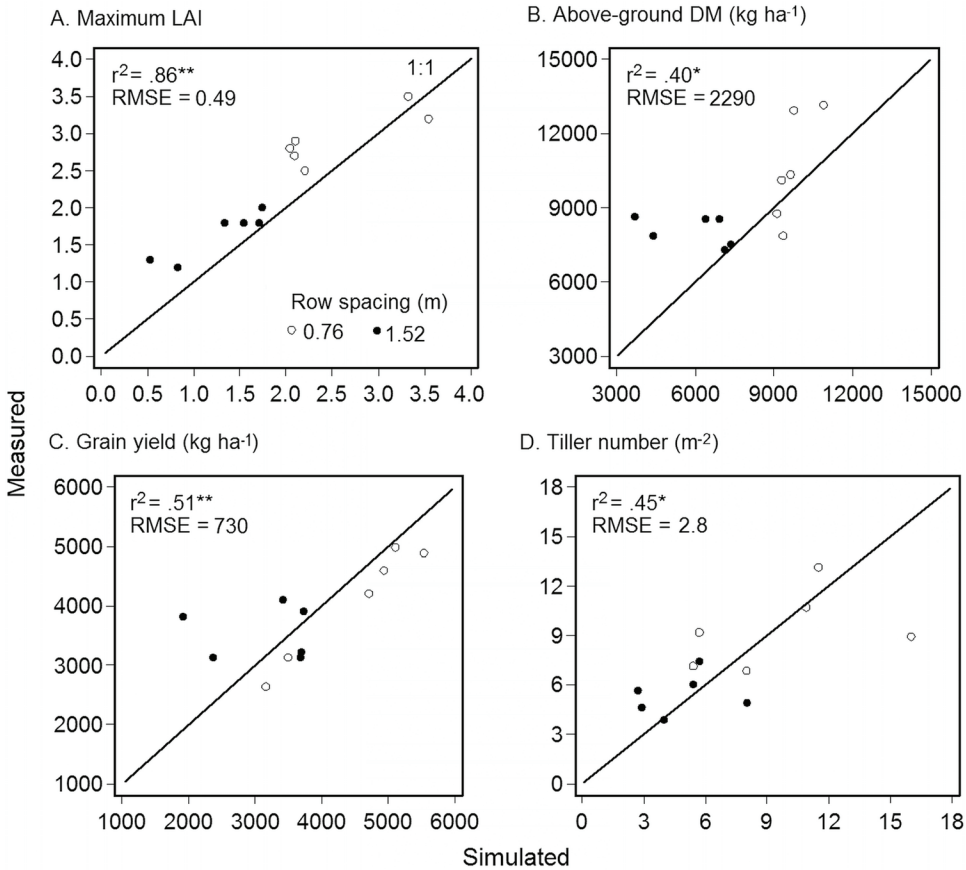

Fig. 2. Comparisons of measured vs. simulated values for a 3-yr series of experiments at Bushland, TX, involving two row spacings and three plant populations. Variables shown are (A) maximum LAI, (B) aboveground dry matter, (C) grain yield, and (D) tiller number. Experimental conditions, management, and results were as reported by Jones and Johnson (1991).

Dwarf-38 having higher yields than the hybrid RS-610 (r^2 = 0.28, $P < 0.05$; Fig. 4). In agreement with Erie et al. (1959), the modeled yield differences among the three N levels (90 to 220 kg ha^{-1} for a single cultivar × irrigation level) were similar to the standard errors of 135 kg ha^{-1} for measurements at the cultivar × irrigation × N level.

Response to irrigation was also simulated for forage sorghum grown at Maricopa, AZ, and showed good agreement for dry matter but poorer agreement for leaf area index at harvest, especially in 2010 (Fig. 5 and Table 4).

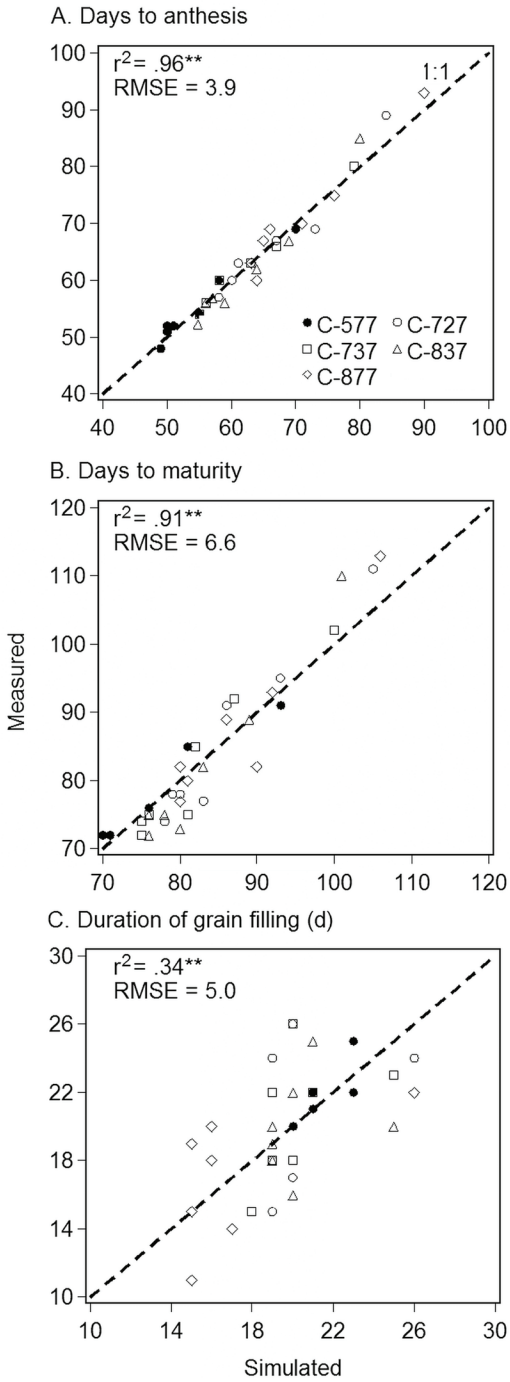

Fig. 3. Comparisons of measured vs. simulated phenology for five Cargill hybrids sown at seven dates in Maricopa, AZ (Ottman et al, 1998) for (A) days to anthesis, (B) days to maturity, and (C) duration of grain filling.

Artificial Defoliation

The model predicted that defoliation would reduce yield in accordance with the magnitude and timing of leaf removal (Fig. 6 and Table 4). Poor prediction for Plainsman in 1959 in part reflected the inability of the model to differentiate between treatments where the upper or lower halves of the leaves were removed.

Tillage and Soil Organic Carbon

Rainfed sorghum and winter wheat production in the semi-arid southern Great Plains is water limited, and no-till practices are recommended to conserve soil moisture and reduce runoff and erosion (Unger, 1994). In simulating a 40-yr series of sorghum–wheat rotation, no-till increased aboveground dry matter by 7% over conventional tillage and increased grain yield by 12% (Fig. 7). The mean sorghum grain yield was 3300 kg ha^{-1} for no-till and 2940 kg ha^{-1} for conventional tillage. Over 7 yr at the same location, Unger (1994) reported a mean of 3910 kg ha^{-1} for no-till and 3480 kg ha^{-1} for a reduced-tillage system. Simulations of both tillage systems showed a long-term reduction in soil-organic matter equivalent to –243 kg ha^{-1} yr^{-1} for no-till and –245 kg ha^{-1} yr^{-1} for conventional tillage.

Atmospheric Carbon Dioxide

Figure 8 shows the modeled responses to [CO_2] of grain yield, season evapotranspiration, and water use efficiency, using the 2006 growth study at Manhattan, KS, to provide crop management information (as applied in Fig. 1). The four simulations in Fig. 8 correspond to the response to [CO_2] as currently specified in the model and for three larger responses. The default (i.e., current model) multiplier effect on RUE is small, only 1.05 at 650 μL L^{-1}, but due to the exponential nature of vegetative plant growth, this effect translated into large effects

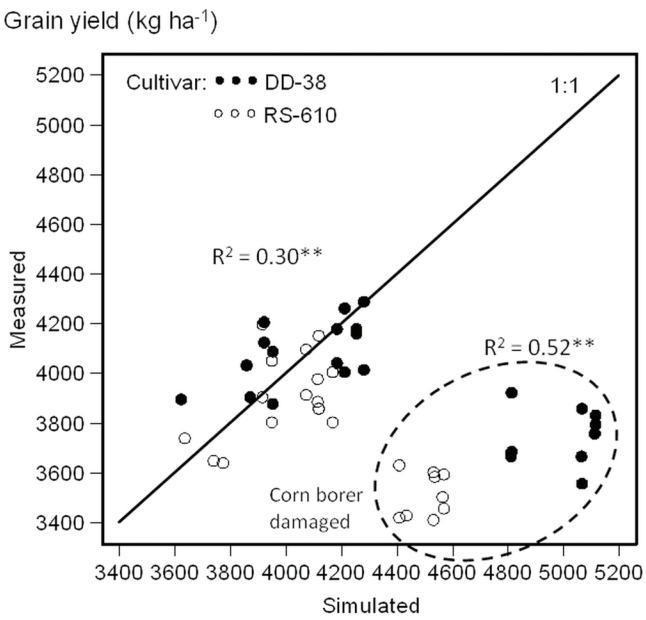

Fig. 4. Comparison of measured vs. simulated grain yield from an irrigation by N experiment at Mesa, AZ, in 1958 (Erie et al., 1959) and involving cultivar Double Dwarf 38 and the hybrid RS-610. Points at the lower right correspond to three irrigation treatments with severe corn borer damage.

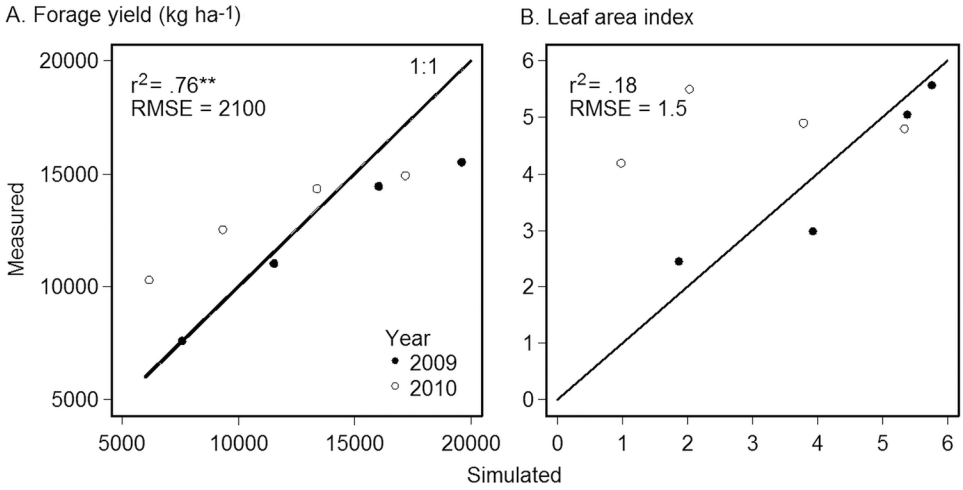

Fig. 5. Comparisons of measured vs. simulated crop response to four irrigation regimes at Maricopa, AZ, in 2009 and 2010 (Ottman, 2010) for (A) forage yield (dry weight) and (B) leaf area index at harvest.

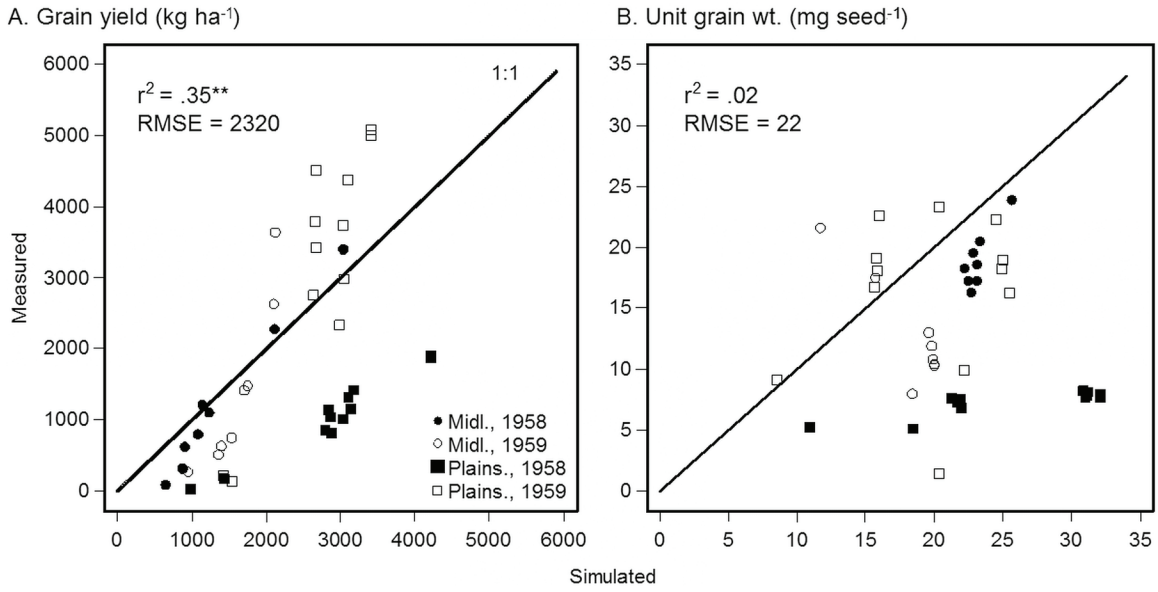

Fig. 6. Comparisons of measured vs. simulated crop response to mid-season defoliations in four experiments at Manhattan, KS, in 1958 and 1959 (Stickler and Pauli, 1961) and involving cultivar Midland and Plainsman for (A) grain yield and (B) unit grain weight.

on growth and yield. For 650 μL L^{-1} [CO_2], the increases in aboveground dry matter and grain yield were both approximately 18% (Fig. 8B and 8C). Increasing the multiplier slightly, produced even greater responses. Thus an increase of the RUE effect to 1.08 (for the 650 μL L^{-1} [CO_2] and the 1.05 linear adjustment), increased the grain yield by 26%.

For the Manhattan, KS, conditions, season evapotranspiration declined with [CO_2], but the effect was less pronounced than the growth effect and showed minimal sensitivity to the RUE multiplier (Fig. 8C). As a result, the simulated increase in water use efficiency was predominantly driven by a greater growth in biomass (Fig. 8D).

DISCUSSION

Overall, the results from this study suggest that the CSM–CERES–Sorghum model can provide credible simulations for sorghum crop growth and development across a range of environments and management practices. Nonetheless, since the examples involved limited calibration to match cultivar traits and did not represent independent test datasets, the model should be tested further for specific applications. Notably, modeled response to soil N was not evaluated in detail, including crop uptake and allocation to grain. A particular concern is that the model code frequently assumes that only the most limiting factor among temperature, N, and water affects a given process.

The poor agreement for duration of grain filling at Maricopa (Fig. 3C) is a concern because this error is likely to affect the estimates for grain yield and unit grain weight. However, due to the relatively short duration of grain filling (mean of 20 d) in this warm environment, a substantial portion of the disagreement may reflect combined errors from measuring time of anthesis and physiological maturity.

In situations where sorghum is sown at low populations or in wide rows, tillers can represent an important crop component for light interception, growth, and yield formation. Based on the limited data from the study of row width and plant population and the recognized difficulty of simulating tiller

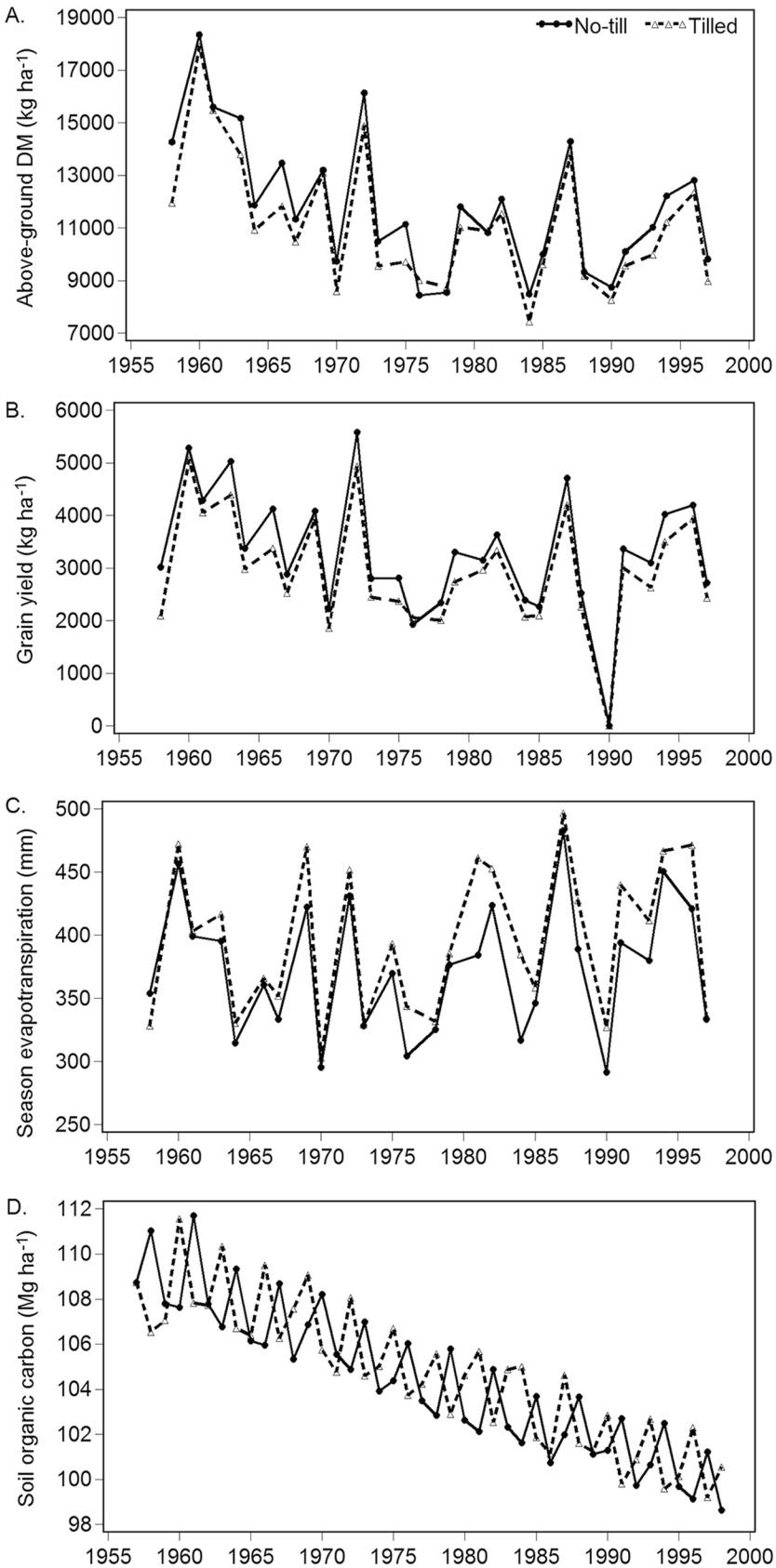

Fig. 7. Results from simulations for a hypothetical sorghum–winter wheat rotation at Bushland, TX, from 1958 to 1999 and comparing no-till vs. tillage. Graphs (A) through (C) are for the sorghum crop only, and (D) is for the end of each cropping year. Variables shown are (A) aboveground dry matter at harvest, (B) grain yield, (C) cumulative evapotranspiration over the season, and (D) total soil organic C including surface residue.

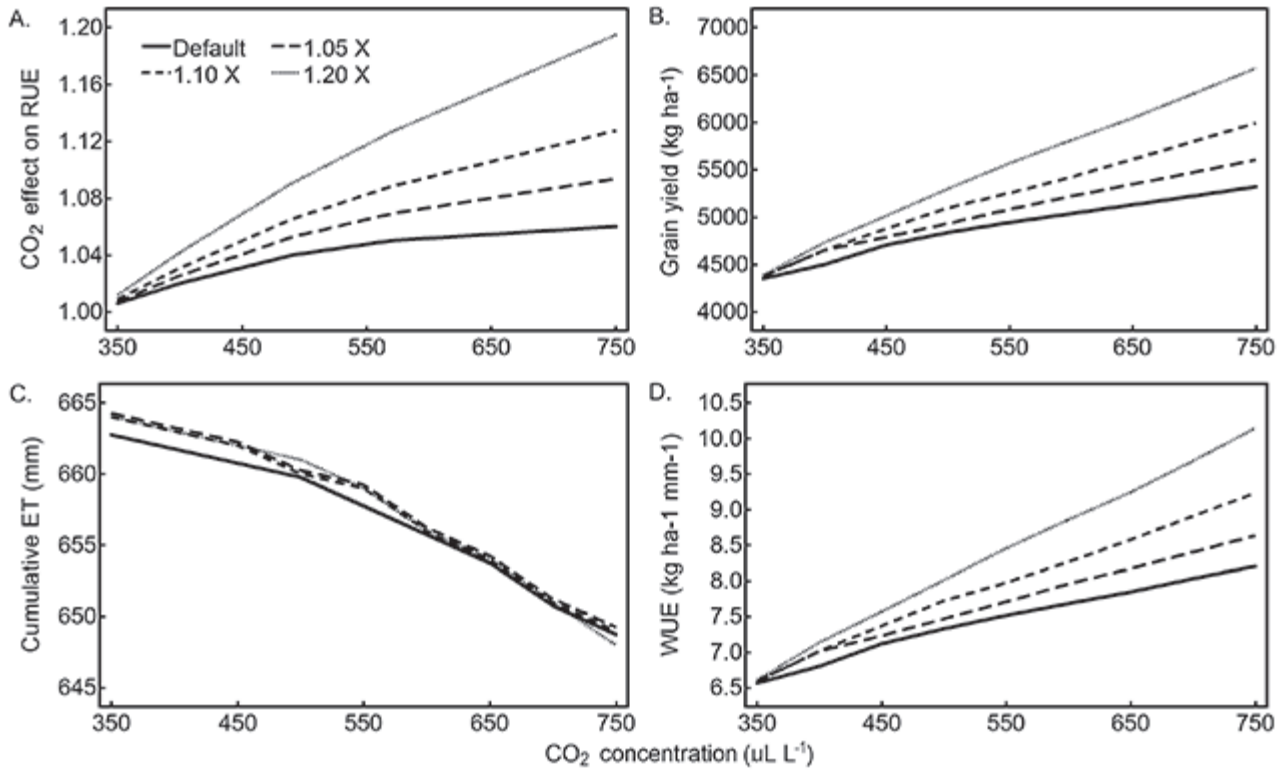

Fig. 8. Simulated responses to atmospheric [CO_2] for a rainfed crop at Manhattan, KS, using the default effect of [CO_2] on RUE plus effects that were equivalent to 1.05, 1.10, or 1.20 times the default response. Variables shown are (A) radiation use efficiency, (B) grain yield, (C) season total evapotranspiration, and (D) water use efficiency.

development (Kim et al., 2010), the assumptions affecting tillering also merit further testing. Similarly, stay-green is not considered in the model although genetic differences in "stay-green" trait affect performance under water deficit conditions (Borrell et al., 2014).

The simulated responses of growth and grain yield to elevated [CO_2] are a direct result of the assumed effect of [CO2] on RUE (Fig. 8a). Thus, correct parameterization of the [CO_2]-effect is essential for climate change research. However, only one set of experiments has characterized sorghum response to [CO_2] under free-air CO_2 enrichment (FACE; Conley et al., 2001), and Bunce (2012) has shown that due to effects of fluctuating [CO_2], which are inherent to field studies, estimates of growth responses may be lower than would occur under constant high [CO_2].

Given interests in using simulation models to examine effects of climate uncertainty (MacCarthy et al., 2010; Grossi et al., 2013; Singh et al., 2014), the temperature responses for growth and development also merit further testing. Singh et al. (2014), citing evidence of Prasad et al. (2006) from sunlit controlled-temperature chambers, argued that the temperature responses of CSM–CERES–Sorghum for growth (PCARB) and grain filling have upper limits that are unrealistically high. However, their analyses appeared to ignore important differences in whether assumed cardinal temperatures are referenced to instantaneous, daily mean, or weighted mean temperatures.

We note that our assessments were constrained by incomplete descriptions of experiments. The most recurrent problems were lack of data on initial soil moisture and N and on crop phenology. These data deficiencies likely contribute to poor model performance where multiple years or locations were considered (e.g., Fig. 5 and 6). Model calibration and evaluation would also benefit from more data on mid-season growth including leaf and tiller numbers and leaf area index. This again emphasizes the importance of collecting complete and comprehensive data, not only for model evaluation, but also as a resource to help understand measured differences among treatments (Hunt et al., 2001; Hoogenboom et al., 2012; White et al., 2013).

CONCLUSION

The CSM–CERES–Sorghum model appears suitable for applications ranging from crop management to potential impacts of sorghum production on soil carbon. As a component of CSM, the model is especially well-suited for comparisons among crops, including examination of cropping sequences. Since our simulations did not include tests with datasets independent of calibrations, further evaluation for specific applications is needed. Potential areas for model improvement based on the responses in the test datasets include tillering, duration of grain filling, and estimation of final grain size. Two topics not explored but that also merit further attention are responses to N and cardinal temperatures assumed for growth and development.

ACKNOWLEDGMENTS

The authors thank the numerous researchers who have contributed to the development of CSM–CERES–Sorghum and its predecessor, CERES–Sorghum, most notably Joe Ritchie. We also acknowledge Scott Staggenborg and Richard Vanderlip who provided data for the simulations. USDA is an equal opportunity provider and employer.

REFERENCES

Alagarswamy, G., U. Singh, and D. Godwin. 1989. Modeling nitrogen uptake and response in sorghum and pearl millet. In: S.M. Virmani, H.L.S. Tandon, and G. Alagarswamy, editors, Modeling the growth and development of sorghum and pearl millet. Res. Bull.12. ICRISAT, Patancheru, Andhra Pradesh. http://oar.icrisat.org/955/ (accessed 10 Feb. 2015). p. 11–12.

Alagarswamy, G., and S.M. Virmani. 1996. Risk analysis of rainfed sorghum production at various levels of nitrogen fertilizer rate with the CERES Sorghum crop simulation model. In: O. Ito et al., editors, Dynamics of roots and nitrogen in cropping systems of the semi-arid tropics. Japan International Research Center for Agricultural Sciences and the International Crops Research Institute for the Semi-Arid Tropics (ICRISAT), Patancheru, Andhra Pradesh, India. p. 603–616.

Alagarswamy, G., D. Reddy, and G. Swaminathan. 1998. Durations of the photoperiod-sensitive and-insensitive phases of time to panicle initiation in sorghum. Field Crops Res. 55:1–10. doi:10.1016/S0378-4290(97)00039-7

Blum, A., and G. Arkin. 1984. Sorghum root growth and water-use as affected by water supply and growth duration. Field Crops Res. 9:131–142. doi:10.1016/0378-4290(84)90019-4

Boote, K.J. 1999. Concepts for calibrating crop growth models. In: G.W. Hoogenboom, P.W. Wilkens, and G.Y. Tsuji, editors, DSSAT Version 3. Vol. 4. Univ. of Hawaii, Honolulu.

Boote, K.J., J.W. Jones, J.W. Mishoe, and R.D. Berger. 1983. Coupling pests to crop growth simulators to predict yield reductions. Phytopathology 73:1581–1587. doi:10.1094/Phyto-73-1581

Borrell, A.K., J.E. Mullet, B. George-Jaeggli, E.J. van Oosterom, G.L. Hammer, P.E. Klein, and D.R. Jordan. 2014. Drought adaptation of stay-green sorghum is associated with canopy development, leaf anatomy, root growth, and water uptake. J. Exp. Bot. 65(21):6251–6263.. doi:10.1093/jxb/eru232

Brouwer, R. 1983. Functional equilibrium-sense or nonsense. Neth. J. Agric. Sci. 31:335–348.

Bunce, J. 2012. Responses of cotton and wheat photosynthesis and growth to cyclic variation in carbon dioxide concentration. Photosynthetica 50:395–400. doi:10.1007/s11099-012-0041-7

Castrignanó, A., V. Di Bari, and M. Stelluti. 1997. Evapotranspiration predictions of CERES-Sorghum model in Southern Italy. Eur. J. Agron. 6:265–274. doi:10.1016/S1161-0301(97)00002-6

Conley, M.M., B.A. Kimball, T.J. Brooks, P.J. Pinter, D.J. Hunsaker, G.W. Wall et al. 2001. CO_2 enrichment increases water-use efficiency in sorghum. New Phytol. 151:407–412. doi:10.1046/j.1469-8137.2001.00184.x

Curry, R., R. Peart, J. Jones, K. Boote, and J. Allen, Jr. 1990. Simulation as a tool for analyzing crop response to climate change. Trans. ASAE 33:981–990. doi:10.13031/2013.31427

Dahlberg, J., J. Berenji, V. Sikora, and D. Latkovic. 2011. Assessing sorghum [*Sorghum bicolor* (L) Moench] germplasm for new traits: Food, fuels and unique uses. Maydica 56:85–92.

Edmeades, G., and T. Daynard. 1979. The relationship between final yield and photosynthesis at flowering in individual maize plants. Can. J. Plant Sci. 59:585–601. doi:10.4141/cjps79-097

Erie, L.J., K. Harris, and F. French. 1959. Water management investigations. Annual Report 1959. U.S. Water Conserv. Lab., USDA, ARS, Phoenix, AZ.

FAOSTAT. 2015. Statistics for broad beans, horse beans, dry. Food and Agric. Organization of the United Nations. http://faostat3.fao.org/compare/E (accessed 22 Apr. 2015).

Francis, C.A. 1970. Effective day lengths for the study of photoperiod sensitive reactions in plants. Agron. J. 62:790–792. doi:10.2134/agronj1970.00021962006200060032x

Gijsman, A.J., G. Hoogenboom, W.J. Parton, and P.C. Kerridge. 2002. Modifying DSSAT crop models for low-input agricultural systems using a soil organic matter-residue module from CENTURY. Agron. J. 94:462–474. doi:10.2134/agronj2002.4620

Godwin, D.C., and U. Singh. 1998. Nitrogen balance and crop response to nitrogen in upland and lowland cropping systems. In: G.Y. Tsuji, G. Hoogenboom, and P.K. Thornton, editors, Understanding options for agricultural production. Kluwer Academic Publ., Dordrecht, the Netherlands. p. 55–78.

Grossi, M.C., F. Justino, C. de L.T.Andrade, E.A. Santos, R.A. Rodrigues, and L.C. Costa. 2013. Modeling the impact of global warming on the sorghum sowing window in distinct climates in Brazil. Eur. J. Agron. 51:53–64. doi:10.1016/j.eja.2013.07.002

Hatfield, J., K. Boote, P. Fay, L. Hahn, C. Izaurralde, B. Kimball et al. 2008. Agriculture. In: P. Backlund et al., editors, The effects of climate change on agriculture, land resources water resources, and biodiversity in the United States. USDA, Washington, DC. p. 21–74.

Hoogenboom, G., J.W. Jones, P.C.S. Traore, and K.J. Boote. 2012. Experiments and data for model evaluation and application. In: J. Kihara, D. Fatondji, J.W. Jones, G. Hoogenboom, R. Tabo, and A. Bationo, editors, Improving soil fertility recommendations in Africa using the Decision Support System for Agrotechnology Transfers (DSSAT). Springer, Dordrecht, the Netherlands. p. 9–18.

Hoogenboom, G., J.W. Jones, P.W. Wilkens, C.H. Porter, K.J. Boote, L.A. Hunt et al. 2011. Decision Support System for agrotechnology transfer. Univ. of Hawaii, Honolulu.

Hunt, L.A., J.W. White, and G. Hoogenboom. 2001. Agronomic data: Advances in documentation and protocols for exchange and use. Agric. Syst. 70:477–492. doi:10.1016/S0308-521X(01)00056-7

Jones, J.W., G. Hoogenboom, C.H. Porter, K.J. Boote, W.D. Batchelor, L.A. Hunt et al. 2003. The DSSAT cropping system model. Eur. J. Agron. 18:235–265. doi:10.1016/S1161-0301(02)00107-7

Jones, O.R., and G.L. Johnson. 1991. Row width and plant density effects on Texas High Plain Sorghum. J. Prod. Agric. 4:613–621. doi:10.2134/jpa1991.0613

Jones, C.A., and J.R. Kiniry. 1986. CERES-Maize: A simulation model of maize growth and development. Texas A&M Univ. Press, College Station.

Jones, C.A., J.T. Richie, J.R. Kiniry, and D.C. Godwin. 1986. Subroutine structure. In: C.A.K. Jones and J.T. Ritchie, editors, CERES-Maize: A simulation model of maize growth and development. Texas A&M Univ. Press, College Station. p. 49–111.

Kim, H.K., E. van Oosterom, M. Dingkuhn, D. Luquet, and G. Hammer. 2010. Regulation of tillering in sorghum: Environmental effects. Ann. Bot. (Lond.) 106:57–67. doi:10.1093/aob/mcq079

Lambers, H. 1987. Growth, respiration, exudation and symbiotic associations: The fate of carbon translocated to the roots. In: P.J.L. Gregory, J.V. Lake, and D.A. Rose, editors, Root development and function. Vol. 30. Cambridge Univ. Press, Cambridge, UK. p. 124–145.

MacCarthy, D.S., P.L. Vlek, A. Bationo, R. Tabo, and M. Fosu. 2010. Modeling nutrient and water productivity of sorghum in smallholder farming systems in a semi-arid region of Ghana. Field Crops Res. 118:251–258. doi:10.1016/j.fcr.2010.06.005

Miller, A.N., and M.J. Ottman. 2010. Irrigation frequency effects on growth and ethanol yield in sweet sorghum. Agron. J. 102:60–70. doi:10.2134/agronj2009.0191

Nix, H. 1976. Climate and crop productivity in Australia. In: S. Yoshida, editor, Climate and rice. IRRI, Los Baños, Philippines. p. 495–507.

Ottman, M.J. 2010. Water use efficiency of forage sorghum grown with sub-optimal irrigation, 2009–2010 forage and grain report. College of Agric., The Univ. of Arizona, Tucson. http://extension.arizona.edu/sites/extension.arizona.edu/files/pubs/az1526d.pdf (accessed 10 Feb. 2015). p. 26–29.

Ottman, M.J., S.H. Husman, R.D. Gibson, and M.T. Rogers. 1998. Planting date and sorghum flowering at Maricopa, 1997. 1998 Forage and grain agriculture report. College of Agric., The Univ. of Arizona, Tucson. http://cals.arizona.edu/pubs/crops/az1059/ (accessed 10 Feb. 2015).

Pachta, C. 2007. Improving irrigated cropping systems on the high plains using crop simulation models. M.Sc. thesis. Dep. of Agronomy, Kansas State Univ., Manhattan.

Porter, C.H., J.W. Jones, S. Adiku, A.J. Gijsman, O. Gargiulo, and J.B. Naab. 2010. Modeling organic carbon and carbon-mediated soil processes in DSSAT v4.5. Oper. Res. 10:247–278.

Prasad, P.V., K.J. Boote, and L.H. Allen. 2006. Adverse high temperature effects on pollen viability, seed-set, seed yield and harvest index of grain-sorghum [*Sorghum bicolor* (L.) Moench] are more severe at elevated carbon dioxide due to higher tissue temperatures. Agric. Forest Meteorol. 139:237–251.

Rami, J.-F., P. Dufour, G. Trouche, G. Fliedel, C. Mestres, F. Davrieux, P. Blanchard, and P. Hamon. 1998. Quantitative trait loci for grain quality, productivity, morphological and agronomical traits in sorghum (*Sorghum bicolor* L. Moench). Theor. Appl. Genet. 97:605–616. doi:10.1007/s001220050936

Ritchie, J.T. 1998. Soil water balance and plant stress. In: G.Y. Tsuji, G. Hoogenboom, and P.K. Thornton, editors, Understanding options for agricultural production. Kluwer Academic Publ., Dordrecht, the Netherlands. p. 41–54.

Ritchie, J.T., and G. Alagarswamy. 1989a. Simulation of sorghum and pearl millet phenology. In: S.M. Virmani, H.L.S. Tandon, and G. Alagarswamy, editors, Modeling the growth and development of sorghum and pearl millet. Res. Bull. 12. ICRISAT, Patancheru, A.P. 502 324, India. http://oar.icrisat.org/955/ (accessed 10 Feb. 2015). p. 24–26.

Ritchie, J.T., and G. Alagarswamy. 1989b. Simulation of growth and development in CERES models. In: S.M. Virmani, H.L.S. Tandon, and G. Alagarswamy, editors, Modeling the growth and development of sorghum and pearl millet. Res. Bull. 12. ICRISAT, Patancheru, A.P. 502 324., India. http://oar.icrisat.org/955/ (accessed 10 Feb. 2015). p. 34–38.

Ritchie, J.T., and D. Godwin. 2000. Documentation of procedures used for development and growth without water or nutrient deficiencies. Michigan State Univ., East Lansing. http://nowlin.css.msu.edu/wheat_book/CHAPTER2.html (accessed 23 Apr. 2015).

Ritchie, J.T., and S. Otter. 1985. Description and performance of CERES-Wheat: A user-oriented wheat yield model In: W.O. Willis, editor, ARS Wheat Yield Project. ARS-38. Natl. Tech. Info. Serv, Springfield, VA. p. 159–175.

Ritchie, J.T., U. Singh, D.C. Godwin, and W.T. Bowen. 1998. Cereal growth, development and yield. In: G.Y. Tsuji, G. Hoogenboom, and P.K. Thornton, editors, Understanding options for agricultural production. Kluwer Academic Publ., Dordrecht, the Netherlands. p. 79–98.

Robertson, M.J., S. Fukai, G.L. Hammer, and M.M. Ludlow. 1993. Modelling root growth of grain sorghum using the CERES approach. Field Crops Res. 33:113–130. doi:10.1016/0378-4290(93)90097-7

Singh, U., J.E. Brink, P.K. Thornton, and C.B. Christianson. 1993. Linking crop models with a geographic information system to assist decision making: A prototype for the Indian Semiarid Tropics. IFDC Paper Ser. P-19. IFDC, Muscle Shoals, AL. http://pdf.usaid.gov/pdf_docs/PNABP796.pdf (accessed 22 Apr. 2015).

Singh, P., S. Nedumaran, P.C.S. Traore, K.J. Boote, H.F.W. Rattunde, P.V.V. Prasad et al. 2014. Quantifying potential benefits of drought and heat tolerance in rainy season sorghum for adapting to climate change. Agric. For. Meteorol. 185:37–48. doi:10.1016/j.agrformet.2013.10.012

Staggenborg, S., and R. Vanderlip. 2005. Crop simulation models can be used as dryland cropping systems research tools. Agron. J. 97:378–384. doi:10.2134/agronj2005.0378

Stickler, F.C., and A.W. Pauli. 1961. Leaf removal in grain sorghum. I. Effects of certain defoliation treatments on yield and components of yield. Agron. J. 53:99–102. doi:10.2134/agronj1961.00021962005300020011x

Teng, P.S., W.D. Batchelor, H.O. Pinnschmidt, and G.G. Wilkerson. 1998. Simulation of pest effects on crops using coupled pest-crop models: The potential for decision support. In: G.Y. Tsuji, G. Hoogenboom, and P.K. Thornton, editors, Understanding options for agricultural production. Kluwer Academic Publ., Dordrecht, the Netherlands. p. 221–226.

Unger, P.W. 1994. Tillage effects on dryland wheat and sorghum production in the Southern Great Plains. Agron. J. 86:310–314. doi:10.2134/agronj1994.00021962008600020019x

Vanderlip, R.L. 1993. How a sorghum plant develops. Kansas State Univ., Manhattan. http://www.ksre.ksu.edu/bookstore/pubs/S3.pdf (accessed 10 Dec. 2014).

White, J.W., G. Hoogenboom, and L.A. Hunt. 2005. A structured procedure for assessing how crop models respond to temperature. Agron. J. 97:426–439. doi:10.2134/agronj2005.0426

White, J.W., L.A. Hunt, K.J. Boote, J.W. Jones, J. Koo, S. Kim et al. 2013. Integrated description of agricultural field experiments and production: The ICASA Version 2.0 Data Standards. Comput. Electron. Agric. 96:1–12. doi:10.1016/j.compag.2013.04.003

White, J.W., J.W. Jones, C. Porter, G.S. McMaster, and R. Sommer. 2010. Issues of spatial and temporal scale in modeling the effects of field operations on soil properties. Oper. Res. 10:279–299.